Molecular Cancer Research

November 2013 • Volume 11 • Number 11 • Pages 1293–1478

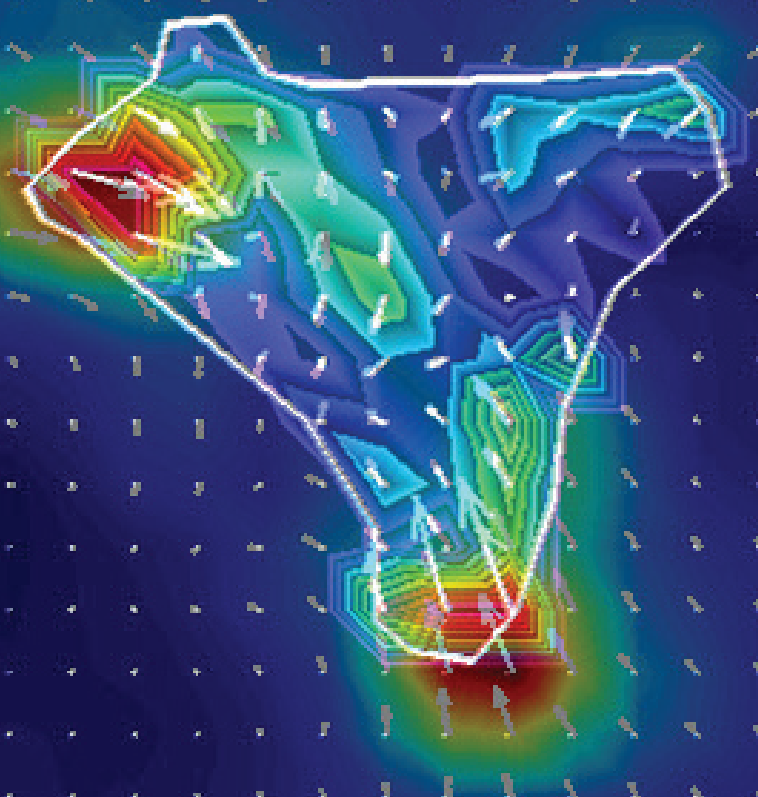

Defining the Molecular Basis of Malignancy and Progression

www.aacrjournals.org

AACR American Association for Cancer Research

Contents

Molecular Cancer Research
Defining the Molecular Basis of Malignancy and Progression
November 2013 • Volume 11 • Number 11

SIGNAL TRANSDUCTION

AC icon indicates Author Choice

For more information please visit www.aacrjournals.org

ABOUT THE COVER

Twist1 overexpression increases the ability of a single prostate cancer cell to exert traction force upon its surrounding. On the cover, a representative deformation field image is superimposed with the corresponding intracellular traction maps of a Myc-CaP prostate cancer cell overexpressing Twist1 using constrained Fourier transform traction cytometry. The colors within the cells represent the absolute magnitude of tractions in Pascals, and the arrows represent the relative magnitude and directions. Prostate cancer cells overexpressing Twist1 exhibited higher cell traction force than isogenic vector control cells. See article by Gajula and colleagues (beginning on page 1387) for more information.

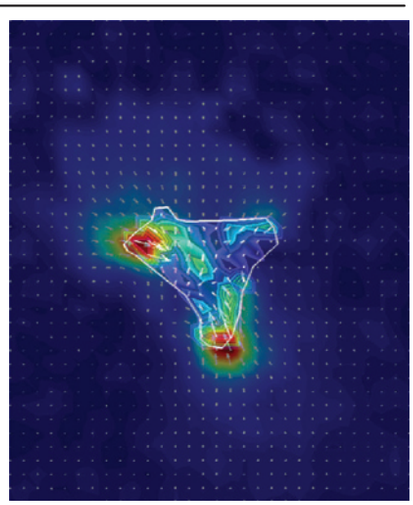

Molecular Cancer Research

Highlights of This Issue

Mol Cancer Res 2013;11:1293.

Molecular Cancer Research **Highlights**

November 2013 • Volume 11 • Number 11

Selected Articles from This Issue

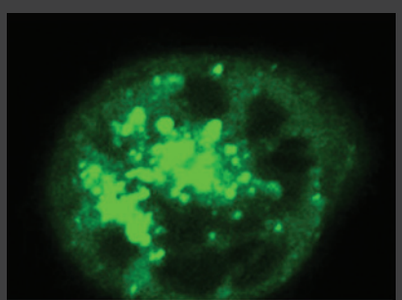

mTOR Inhibition Enhances the Efficacy of Aurora Inhibitors

Liu *et al.* **Page 1326**

Aurora kinase overexpression is known to be important for tumor development and progression. Although Aurora kinase inhibitors have significant therapeutic potential, their single-agent efficacy appears to be uniformly modest and needs improvement. Liu and colleagues reveal that AML cells with polyploidy, induced by Aurora kinase inhibition, have elevated glycolytic metabolism and are sensitive to metabolic deprivation or glycolytic inhibitors like 2DG (2-deoxy-D-glucose). Moreover, mTOR inhibition suppressed the metabolism of polyploidy cells and promoted an autophagic response and apoptotic death. Notably, p62 (*SQSTM1*) was demonstrated to be a metabolic regulator in polyploidy cells. These findings indicate that mTOR inhibition enhances the efficiency of Aurora kinase inhibitors and provide a novel treatment strategy against AML.

miR-106a in Ovarian Serous Carcinoma

Liu *et al.* **Page 1314**

High-grade serous ovarian cancers (HGSOC) are poorly differentiated and fast-growing tumors. The molecular mechanism for HGSOC differentiation remains unknown. microRNAs play an important role in early development and cell differentiation. Therefore, Liu and colleagues performed global microRNA profiling, which revealed that miR-106a is frequently upregulated in HGSOC. Importantly, miR-106a overexpression in normal and malignant cell lines resulted in increased cellular proliferation, expanded side populations, and increased tumor initial/stem cell populations both *in vitro* and *in vivo*. Furthermore, miR-106a–mediated tumor differentiation was largely contributed by repression of p130 (*RBL2*), an RB tumor suppressor family member. As such, downregulation of *RBL2* by miR-106a represents a major molecular event that may underwrite the aggressive and poorly differentiated nature of HGSOC.

Twist Box is Needed for Prostate Cancer Metastasis

Gajula *et al.* **Page 1387**

Twist1 is a prime player during development and is a master transcriptional regulator of the epithelial–mesenchymal transition that promotes cancer metastasis. Gajula and colleagues demonstrate three relevant findings for prostate cancers that overexpress Twist1: First, Twist1 leads to elevated cytoskeletal stiffness and traction forces at the migratory edge of cell collections; Second, the Twist box domain is required for Twist1-induced prometastatic processes *in vitro* and metastases *in vivo*; and Third, Hoxa9 is a novel Twist1 transcriptional target that is required for Twist1-induced prometastatic phenotypes. Thus, targeting the Twist box domain and Hoxa9 may effectively limit prostate cancer metastatic potential.

LOXL2 Drives Fibroblast Activation

Barker *et al.* **Page 1425**

Fibroblast interactions in the extracellular matrix are critical for normal tissue homeostasis. Cancer-associated fibroblasts are a heterogeneous population of cells that support malignant progression through multiple mechanisms. Barker and colleagues discovered that tumor-derived and secreted lysyl oxidase-like-2 (LOXL2) is vital for stromal fibroblast activation in orthotopically grown mammary tumors. A reduction in fibroblast-associated α-smooth muscle actin was demonstrated using genetic and antibody inhibitory approaches directed against LOXL2. Tumor-derived or recombinant LOXL2 promoted fibroblast properties necessary for metastasis. Importantly, it was shown that LOXL2 fibroblast activation was dependent on integrin-mediated focal adhesion kinase signaling. This novel function of LOXL2 highlights the potential for targeted approaches to prevent tumor progression.

Genomics

Molecular Cancer Research

The Twist Box Domain Is Required for Twist1-induced Prostate Cancer Metastasis

Rajendra P. Gajula[1], Sivarajan T. Chettiar[1], Russell D. Williams[1], Saravanan Thiyagarajan[1], Yoshinori Kato[2,4,7], Khaled Aziz[1], Ruoqi Wang[5], Nishant Gandhi[1], Aaron T. Wild[1], Farhad Vesuna[4], Jinfang Ma[5], Tarek Salih[1], Jessica Cades[1,2], Elana Fertig[3], Shyam Biswal[5], Timothy F. Burns[9], Christine H. Chung[2], Charles M. Rudin[2], Joseph M. Herman[1,2], Russell K. Hales[1], Venu Raman[2,4,7], Steven S. An[5,7,8], and Phuoc T. Tran[1,2,6,7]

Abstract

Twist1, a basic helix-loop-helix transcription factor, plays a key role during development and is a master regulator of the epithelial–mesenchymal transition (EMT) that promotes cancer metastasis. Structure–function relationships of Twist1 to cancer-related phenotypes are underappreciated, so we studied the requirement of the conserved Twist box domain for metastatic phenotypes in prostate cancer. Evidence suggests that Twist1 is overexpressed in clinical specimens and correlated with aggressive/metastatic disease. Therefore, we examined a transactivation mutant, Twist1-F191G, in prostate cancer cells using *in vitro* assays, which mimic various stages of metastasis. Twist1 overexpression led to elevated cytoskeletal stiffness and cell traction forces at the migratory edge of cells based on biophysical single-cell measurements. Twist1 conferred additional cellular properties associated with cancer cell metastasis including increased migration, invasion, anoikis resistance, and anchorage-independent growth. The Twist box mutant was defective for these Twist1 phenotypes *in vitro*. Importantly, we observed a high frequency of Twist1-induced metastatic lung tumors and extrathoracic metastases *in vivo* using the experimental lung metastasis assay. The Twist box was required for prostate cancer cells to colonize metastatic lung lesions and extrathoracic metastases. Comparative genomic profiling revealed transcriptional programs directed by the Twist box that were associated with cancer progression, such as Hoxa9. Mechanistically, Twist1 bound to the Hoxa9 promoter and positively regulated Hoxa9 expression in prostate cancer cells. Finally, Hoxa9 was important for Twist1-induced cellular phenotypes associated with metastasis. These data suggest that the Twist box domain is required for Twist1 transcriptional programs and prostate cancer metastasis.

Implications: Targeting the Twist box domain of Twist1 may effectively limit prostate cancer metastatic potential.
Mol Cancer Res; 11(11); 1387–400. ©2013 AACR.

Introduction

Prostate cancer is the most common cancer diagnosed in men in the United States and is responsible for the second most cancer deaths in men (1). Patterns of disease failure in prostate cancer suggest understanding the determinants that confer progression of localized presentations to metastatic disease will result in the largest therapeutic gains (2).

One mechanism by which cancer cells may acquire the characteristics necessary for metastasis is the epithelial–mesenchymal transition (EMT). EMT is a transcriptional program, crucial in early embryonic development that is coopted by some cancer cells to facilitate aggressive and metastatic behavior (3). Twist1 is a basic helix-loop-helix (bHLH) multidomain transcription factor which directly mediates EMT by transcriptional activation and repression of E-box-regulated target genes (4, 5). A role for TWIST in prostate cancer pathogenesis has been suggested (6, 7), but the role of EMT and Twist1 in prostate cancer disease

Authors' Affiliations: [1]Departments of Radiation Oncology and Molecular Radiation Sciences, and [2]Oncology; [3]Division of Biostatistics and Bioinformatics, Department of Oncology, Sidney Kimmel Comprehensive Cancer Center; [4]Division of Cancer Imaging Research, The Russell H. Morgan Department of Radiology and Radiological Science; [5]Department of Environmental Health Sciences, Johns Hopkins Bloomberg School of Public Health; [6]Departments of Urology and [7]In Vivo Cellular and Molecular Imaging Center, Johns Hopkins University School of Medicine; [8]Physical Sciences in Oncology Center, Johns Hopkins University, Baltimore, Maryland; and; [9]Division of Hematology-Oncology, Department of Medicine, Hillman Cancer Center, University of Pittsburgh, Pittsburgh, Pennsylvania

Note: Supplementary data for this article are available at Molecular Cancer Research Online (http://mcr.aacrjournals.org/).

R.P. Gajula and S.T. Chettiar contributed equally to this work.

Corresponding Author: Phuoc T. Tran, Department of Radiation Oncology & Molecular Radiation Sciences, Sidney Kimmel Comprehensive Cancer Center, Johns Hopkins Hospital, 1550 Orleans Street, CRB2 Rm 406, Baltimore, MD 21231. Phone: 410-614-3880; Fax: 410-502-1419; E-mail: tranp@jhmi.edu

doi: 10.1158/1541-7786.MCR-13-0218-T

progression and metastasis is just now being explored (8, 9). The critical domains of Twist1 and the crucial Twist1 downstream transcriptional targets required for increased tumorigenicity and aggressive metastatic phenotypes in prostate cancer are unknown. The carboxyl-terminal Twist box is a highly conserved domain among Twist1 orthologues for which little functional information in the context of cancer phenotypes is known (5). A greater understanding of the structure–function relationships and downstream targets of Twist1 may allow for an increased appreciation of the mechanisms responsible for Twist1-induced metastasis and may facilitate more precise inhibitory strategies of Twist1 as a therapeutic maneuver in cancer.

Here, we used a single amino acid substitution mutation, Twist1 codon 191 phenylalanine-to-glycine (F191G), to study the role of the Twist box for Twist1-induced aggressive cellular and metastatic phenotypes in prostate cancer cells. Isogenic androgen-dependent, Myc-CaP (10), and androgen-independent, PC3, cell lines overexpressing Twist1 or the Twist box mutant showed specific requirements for the Twist box during Twist1-induced metastasis of prostate cancer cells. Gene expression profiling revealed transcriptional programs directed by the Twist box that were associated with cancer metastasis. Finally, we show that Twist1 directly regulates one such target, *Hoxa9*, which is partially required for Twist1-induced prostate cancer prometastatic phenotypes.

Materials and Methods

Plasmids, antibodies, and reagents

pBABE-Twist1-puro or –hygro (11) was used to construct the *Twist1-F191G* mutant using the QuikChange Site-Directed Mutagenesis Kit (Stratagene) and confirmed by sequencing. Antibodies used were: Twist (Twist2C1a; sc-81417, Santa Cruz Biotechnology), E-cadherin (ab53033, Abcam), vimentin (ab92547), ZO-1 (5406, Cell Signaling Technology), β-actin (A5316, Santa Cruz Biotechnology), c-Myc (N-term; 1472-1, Epitomics), horseradish peroxidise-conjugated secondary antibodies (Invitrogen), and Alexa flour 488 conjugated secondary antibodies (Invitrogen). *Hoxa9* shRNA retroviral constructs were purchased and used as directed by Origene (cat #TG500979).

Cell line and culture conditions

PC3 and 22RV1 were obtained from American Type Culture Collection. Myc-CaP was a kind gift from Dr. John Isaacs (Johns Hopkins University, Baltimore, MD; ref. 10). Growth media: Myc-CaP, Dulbecco's modified Eagle medium (Invitrogen); PC3, Hams F12K (Invitrogen); and 22RV1, RPMI-1640 (Invitrogen). Cell line identity confirmed by short tandem repeat profiling and mycoplasma tested. All media were supplemented with 10% FBS and penicillin (100 U/mL), streptomycin (0.1 mg/mL). Cells were maintained at 37°C in a humidified incubator with 5% CO_2 in air.

Retroviral experiments

Retroviral production used ecotropic and amphotropic Phoenix packaging lines. Myc-CaP cells were transduced with pGFP-V-RS-based shRNA contructs from Origene as described above or with scrambled control vector for two successive times over a 36-hour period followed by selection with 1 mg/mL puromycin and passaged once 80% confluent.

Luciferase promoter reporter assay

Subconfluent cells were transfected using Lipofectamine 2000 (Invitrogen) with 200 ng of firefly luciferase reporter gene construct (100 ng was used for *SNAI2* reporter assays), 100 ng of the pRL-SV40 *Renilla* luciferase construct, and 500 ng of the Twist1 or Twist1-F191G–mutant expression construct. Cell extracts were prepared 36 hours after transfection in passive lysis buffer, and the reporter activity was measured using the Dual-Luciferase Reporter Assay System (Promega).

Wound-healing migration assay

Two-dimensional migration assay was conducted using a scratch/wound model. Cells were grown in 6-well plates for 24 hours to confluence. PC3 cells were treated with 500 pmol/L TGF-β at the time of wounding. Multiple scratch wounds were created using a P-20 micropipette tip and cells fed with fresh complete media. Five representative fields of the wound were marked and images were taken at 0 and 24 hours after wounding. Relative wound closure is calculated from the remaining wound area normalized to the initial wound area using ImageJ software (NIH Image).

Biophysical assays

Fourier transform traction microscopy (FTTM) was used to measure the contractile stress arising at the interface between each adherent cell and its substrate as described (12). Briefly, cells were plated sparsely on elastic collagen type I coated gel blocks. Images of fluorescent microbeads (0.2 μm in diameter, Molecular Probes) embedded near the gel apical surface was taken at different times with cell-free reference (traction-free) images. The displacement field between a pair of images was then obtained by identifying the coordinates of the peak of the cross-correlation function (13, 14). From the displacement field and known elastic properties of the gel (Young's modulus of 1 kPa with a Poisson's ratio of 0.48), the cell traction field was computed. The computed traction field was used to obtain net contractile moment, which is a scalar measure of the cell's contractile strength, expressed in pico-Newton meters (pNm).

Magnetic twisting cytometry (MTC) was used to measure material properties of the cytoskeleton as described (15, 16). In brief, cells were plated at 150,000 cells/cm^2 on coated collagen type I plastic wells (96-well Removawell, Immulon II: Dynetech) at 500 ng/cm^2. After scratching with a 200-μL pipette tip and the indicated time, ferrimagnetic microbeads were functionalized to the cytoskeleton, and both stiffness, g' and loss modulus g'', were measured over a physiologic range of frequency (f) expressed in Pascal per nm (Pa/nm).

Matrigel invasion assay

The invasion potential was assessed using Chemicon cell invasion assay kit (Millipore) as directed by the

manufacturer. Of note, 8 μmol/L Transwells with Matrigel were used for the assay. Serum-starved 0.5 to 1 × 10^6 cells (12–16 hours) in 300 μL were seeded in upper chambers, whereas lower wells were filled with 500 μL of 10% FBS complete medium. Invading cells on the lower surface were fixed and stained. The stain is dissolved in 200 μL of 10% acetic acid and measured at 570 nm. Invasive potential is derived by normalizing with the readings from blank Transwell inserts.

Immunohistochemistry, Immunofluorescence, and Western blotting

Immunohistochemistry (IHC), immunofluorescence, and Western blotting were conducted as described previously (17).

Anoikis assay and apoptosis assessment

Anoikis resistance was measured using a modified protocol (18). Cells were grown in normal attachment and ultra-low attachment (Corning) in 6-well plates. Twenty-four hours later, cells were blocked in 5% FBS and stained with Alexa Fluor 488 conjugated AnnexinV followed by propidium iodide staining (50 μg/mL; Invitrogen). Cells were enumerated on a BD FACS Caliber (BD Biosciences), and analysis was done using FlowJo analysis software. All conditions were $n = 4$ and two replicates per experiment.

Clonogenic survival and soft agar colony formation assays

Clonogenic survival was conducted as previously described (19). Soft agar clonogenic assays used 6-well plates precoated with 1 mL of basal 0.6% agarose in complete media and overlaid with 2 mL of cells (5 × 10^3 cells/mL) mixed with 0.3% agarose in complete media and allowed to solidify. The wells were constantly fed with complete media to prevent drying of agarose, and then after 10 to 15 days of incubation, colonies were scored under phase contrast microscopy. All conditions were repeated at least twice with 3 wells per experiment.

Animal models and histology

All procedures were carried out in accordance with the Johns Hopkins Animal Care and Use Committee, maintained under pathogen-free conditions, and given food and water *ad libitum*. For the subcutaneous tumor graft assay, 100 μL of PBS and Matrigel (BD Biosciences) mixed 1:1 containing 0.5 to 2 × 10^6 cells were injected subcutaneously into both the flanks of 8-week-old male FVB/N or athymic nude mice. Tumors measured 3 times weekly and volume calculated: length × width × height × π/6. Tumor growth delay is the difference between the quadrupling times of untreated versus treated tumors. For the experimental lung metastasis assay, 100 μL of PBS containing 5 × 10^5 cells were injected into athymic nude mice via the tail vein. After 4 weeks, the mice were sacrificed, necropsies conducted to score surface lung tumors and extrathoracic metastases.

Microarray data acquisition and analysis

Microarrays were conducted using GeneChip WT cDNA Synthesis and amplification Kit and WT terminal labeling Kit (Affymetrix). The labeled ssDNA was hybridized to the GeneChip Mouse Gene 1.0 ST array (Affymetrix), washed with the Fluidics station 450, and array scanning was conducted as previously described. Arrays were normalized using the Robust Multichip Average in the oligo Bioconductor package at the transcript level. Genes and gene sets with Benjamini–Hochberg $P < 0.05$ were considered statistically significant. Gene set enrichment analysis (GSEA) was conducted using the C2 Curated Gene Sets collection from the Molecular Signature Database 3.0 and statistical comparisons by Fisher Exact test. More detailed description of the analysis and R code used for this analysis are included as Supplementary Materials and Methods.

Chromatin immunoprecipitation

Chromatin immunoprecipitation (ChIP) was conducted using a SimpleChIP Enzymatic IP Kit (Cell Signaling Technology). See Supplementary Materials and Methods for details.

SYBR-green quantitative RT-PCR and prostate cancer cDNA arrays

The iTaq Universal SybrGreen Master Mix (BioRad) was used according to the manufacturer's instructions. Human normal prostate and prostate cancer qPCR tissue arrays and *TWIST1* qPCR oligos were purchased from OriGene. All relevant clinical information can be found in http://www.origene.com/qPCR/Tissue-qPCR-Arrays.aspx.

Statistical analysis

Statistical analysis was carried out using GraphPad Prism v5.04 (GraphPad Software). Paired comparisons were tested using the Mann–Whitney test or Fisher exact test. Throughout this study: *, $P < 0.05$; **, $P < 0.01$; and ***, $P < 0.001$.

Results

TWIST1 is overexpressed in prostate cancer and correlates with aggressive and metastatic disease

TWIST1 expression in prostate cancers was analyzed from 14 independent microarray datasets constituting 1,013 prostate samples (20–32) using Oncomine. Ten of the 14 datasets and the aggregate analysis showed *TWIST1* overexpression in prostate cancers (Fig. 1A, $P = 0.002$ for aggregate). Further analysis of one of these microarray studies (20) showed that *TWIST1* overexpression correlated with metastatic disease (Fig. 1B; $P < 0.000001$).

This microarray data were validated using quantitative PCR (qPCR) for *TWIST1* on human prostate cancer samples. Cancer samples ($n = 107$) screened by qPCR confirmed that *TWIST1* was overexpressed in prostate cancer (40/107 or 37% showed ≥3-fold upregulation, 18/107 or 17% ≥10-fold overexpression, and some cases ≥50-fold overexpression; Fig. 1C; $P < 0.0001$). Similar to the microarray data, *TWIST1* overexpression was directly correlated with prostate cancer aggressiveness as determined by

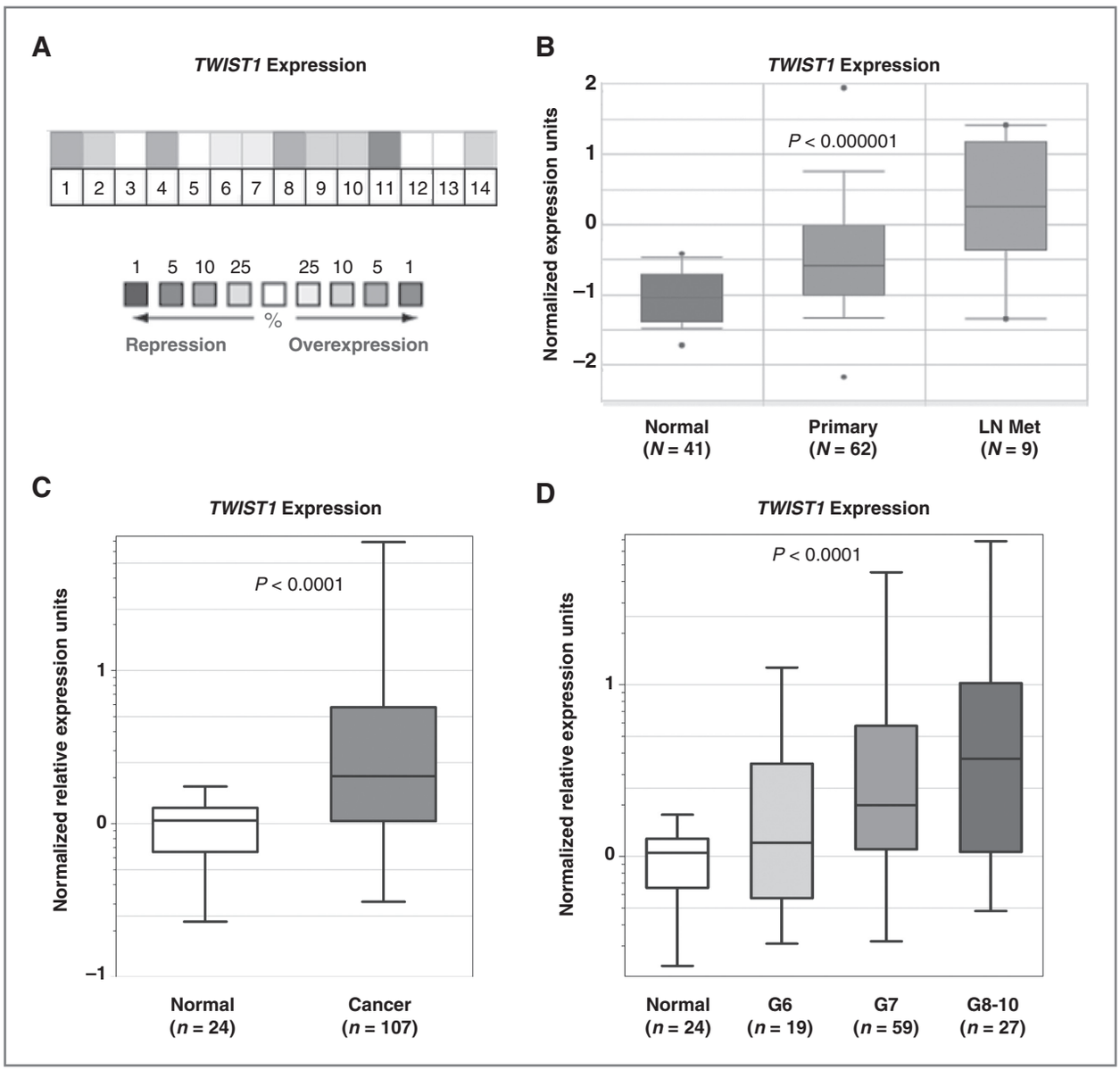

Figure 1. *TWIST1* is overexpressed in human prostate cancers and correlates with more aggressive and metastatic disease. A, human prostate cancer samples ($n = 700$) compared against normal prostate ($n = 313$) from 14 independent microarray datasets for *TWIST1* expression using Oncomine. The heatmap contains individual studies (20–32). The heatmap intensity corresponds to percentile overexpression (right direction) or repression (left direction). The median rank across all 14 datasets shows that *TWIST1* is overexpressed in human prostate cancer, $P = 0.002$. B, analyzing study #2 (20) from A showed that *TWIST1* overexpression correlates with metastatic disease, $P < 0.000001$. C, we validated this microarray analysis by conducting qPCR on primary human prostate samples for *TWIST1*. *TWIST1* mRNA is overexpressed in human prostate cancer ($n = 107$) compared with normal prostate ($n = 24$), $P < 0.0001$ by Mann–Whitney *t* test. D, analysis of data from C broken down by Gleason score shows that *TWIST1* overexpression correlates with increasing Gleason score, $P < 0.0001$ using one-way ANOVA.

Gleason score (Fig. 1D; $P < 0.0001$). These data agreed with prior studies that showed *TWIST1* overexpression in human prostate cancer and correlation with prostate cancer disease aggressiveness and metastasis (7, 33).

The Twist box domain is required for full transcriptional activity of Twist1 in prostate cancer cells

Twist1 has four domains: (i) a Twist1 domain that is highly conserved among human and mice; (ii) a glycine rich region; (iii) bHLH domain; and (iv) the Twist box (or WR domain). The Twist box is identical between mouse, human, frog, zebra fish, and jellyfish species and is located in the last 23 residues of the mouse polypeptide. The Twist box has been shown to be necessary and sufficient to transactivate E-box containing heterologous reporter constructs *in vitro* (34). We generated a site-specific Twist box mutant by mutating a critical Phe-191 to Gly, referred to as Twist1-F191G (Fig. 2A). This Twist1-F191G mutant had

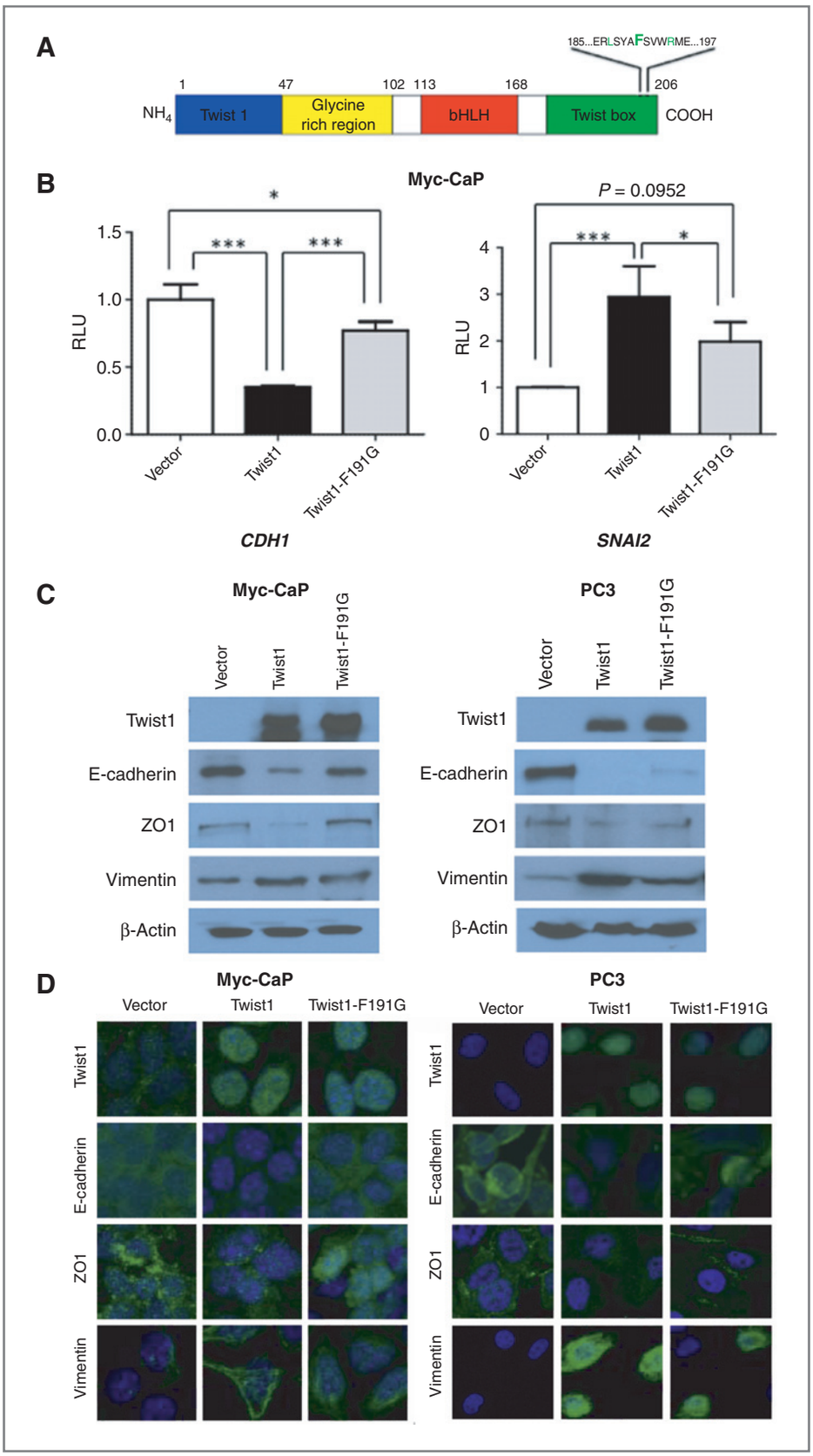

Figure 2. The Twist box mutant is deficient for Twist1 transcriptional activity and displays an attenuated EMT cellular marker profile in prostate cancer cells. A, a schematic of Twist1 protein structure and the position 191 phenylalanine site-specific mutant examined (this schematic is not to scale). Key functional residues required for transcriptional transactivation in the Twist box, L-187, F-191, and R-195, are shown in green. We created constructs overexpressing the Twist1-F191G mutant which has the substitution of phenylalanine-191 for glycine. B, Twist1 promoter reporter assays show that the Twist1-F191G mutant is defective for transcriptional activity. Myc-CaP cells were transiently transfected with expression vectors for the firefly luciferase-linked human E-cadherin gene (*CDH1*) promoter construct and a *Renilla* luciferase reporter vector for normalization of transfection efficiency. After 36 hours, cell extracts were assayed for luciferase and *Renilla* activity and showed *Twist1* overexpression repressed transcription from the E-cadherin gene promoter, but the Twist1-F191G mutant was attenuated for this function (***, $P < 0.001$; and *, $P < 0.05$ by Mann–Whitney test). Similar reporter assays were conducted using a SLUG gene (*SNAI2*) promoter construct and showed that the Twist1-F191G mutant had no ability to transactivate transcription compared with wild-type Twist1 overexpression (***, $P < 0.001$ by Mann–Whitney test). Each bar represents values from five to six independent experiments conducted in triplicate. Bars represent column mean; error bars ±SEM. Western blot analysis was conducted for Twist1 expression in (C) Myc-CaP (left) and PC3 (right) cells stably expressing Vector and overexpressing similar levels of Twist1 or Twist1-F191G with β-actin used as a loading control. Epithelial and mesenchymal markers were also assessed by (C) Western blotting and (D) immunofluorescence for Twist1, E-cadherin, ZO-1, and vimentin in Myc-CaP (left) and PC3 (right) cells.

been shown previously to be deficient for transactivation of E-box containing reporter constructs in mesenchymal cells (34), but has not been examined in epithelial cancer cells. In Myc-CaP androgen-dependent prostate cancer cells, Twist1 overexpression significantly repressed *CDH1* (Fig. 2B, left, $P < 0.001$) promoter activity (35) and increased *SNAI2* (Fig. 2B, right, $P < 0.001$) promoter activity. Twist1-F191G was found to be defective for both repression and activation in these assays and significantly different from Twist1 (Fig. 2B; $P < 0.05$ for both). There was some suggestion that Twist1-F191G was more defective for activation than repression, as Twist1-F191G was still able to repress the *CDH1* promoter to some extent but could not activate the *SNAI2* promoter as compared with Vector control (Fig. 2B, left, $P < 0.05$ and right, $P = 0.0952$). Similarly, in HEK 293 cells, Twist1 repressed *CDH1* promoter activity, whereas Twist1-F191G only partially repressed the *CDH1* promoter activity compared with Twist1 wild-type (Supplementary Fig. S1A, both $P < 0.001$). Neither Twist1 nor Twist1-F191G seemed to alter expression from the *SNAI2* promoter in HEK 293 cells, which is not surprising as this cell line is of likely mesenchymal origin (Supplementary Fig. S1B; all $P>0.05$). These reporter assay data were concordant with levels of the endogenous *Cdh1* and *Snai2* genes and respective gene products when Myc-CaP cells overexpressed Twist1 or Twist1-F191G stably (Fig. 2C and Supplementary Fig. S1C–E). Twist1-F191G bound the *Cdh1* promoter as well as Twist1 wild-type in Myc-CaP cells according to ChIP-qPCR (Supplementary Fig. S1F). These results suggest that the Twist box domain is required for the full transcriptional activity of Twist1.

The Twist box mutant is partially defective for induction of EMT markers in prostate cancer cells

Metastasis is a complex series of discrete events that a neoplastic cell must traverse (36). These serial events include: loss of cell-to-cell adhesion, migration and invasion into the local extracellular matrix, intravasation into the vasculature, resistance to anoikis, extravasation into the parenchyma of distant tissues, and then colonization into a macroscopic metastatic tumor. To ascertain the role of the Twist box domain in a subset of these metastatic steps *in vitro* and *in vivo*, stable isogenic cell lines expressing Twist1 and Twist1-F191G in Myc-CaP and PC3 prostate cancer cells were established (Western blot analysis, Fig. 2C; and immunofluorescence, Fig. 2D, top row and Supplementary Fig. S2A and S2B). Consistent with an EMT marker profile, stable Twist1 overexpression led to downregulation of epithelial markers E-cadherin and ZO-1 in Myc-CaP cells and in PC3 cells and upregulation of the mesenchymal marker vimentin in both Myc-CaP and PC3 cells (Western blotting and immunofluorescence shown in Fig. 2C and D and qPCR shown in Supplementary Figs. S1C and S3A). The Twist box mutation, Twist1-F191G, resulted in a reduced ability to downregulate E-cadherin and ZO-1 and upregulate vimentin in Myc-CaP cells (Fig. 2C and D and Supplementary Figs. S1C and S3A). A similar, but less dramatic loss of an EMT marker profile was seen with PC3 cells stably overexpressing Twist1-F191G (Fig. 2C and D; Supplementary Fig. S2C and S2D show immunofluorescence quantification of PC3 cells; and Supplementary Fig. S3B and S3C show qPCR for *CDH1* and *VIM*). The findings from these prostate cancer cell lines overexpressing Twist1 and Twist1-F191G suggest that the Twist1 box domain is required for Twist1 to induce a full EMT marker profile.

Twist1 overexpression increases cellular motility that is partially defective in the Twist1-F191G mutant

We next examined Twist1-induced cell migration and correlates of cell mechanics using the scratch/wound-healing model. For this study, we made a scratch into an ensemble of confluent Myc-CaP cells (Fig. 3A) and measured the spatiotemporal changes in forced motions of microbeads anchored to the cytoskeleton through integrin cell adhesion receptors (15, 16). Using MTC, we measured cytoskeletal stiffness (g') and internal friction (g'') before, immediately after, and 24-hours after making a scratch. Over five decades of frequency, we found no differences in stiffness g' and friction g'' between isogenic Myc-CaP cell ensembles (Twist1 vs. Vector) before or immediately after a scratch (Supplementary Fig. S4A and S4B). By 24 hours, however, Twist1-overexpressing cells infiltrated more into the site of the scratch wound than Vector control cells (Fig. 3A) and showed appreciably higher cytoskeletal stiffness (Fig. 3B and Supplementary Fig. S4c) and friction (Fig. 3C and Supplementary Fig. S4C). At 24-hour after making a scratch, Twist1-overexpressing cell ensembles exhibited a 1.6-fold higher stiffness than Vector control ensembles (Fig. 3D). Most striking was the greatest differences of cytoskeletal stiffness between Twist1 and Vector control cell ensembles were localized at the leading migratory front (Fig. 3A and E). Twist1-overexpressing cell ensembles had progressively decreasing cytoskeletal stiffness with increasing distance from the leading migratory edge (1st > 2nd > 3rd > 4th cell layers; Fig. 3A and E).

We then directly assessed the requirement of the Twist box domain for Twist1-induced cell invasive potential using the scratch/wound-healing assay *in vitro.* Importantly, Twist1 overexpression did not increase the proliferative potential of Myc-CaP or PC3 cells (Supplementary Fig. S5). Myc-CaP cells overexpressing Twist1 migrated 2.5-fold faster than Vector control Myc-CaP cells (Fig. 3F and G, $P < 0.05$). The Twist1-F191G–overexpressing cells were significantly less migratory than Twist1-overexpressing cells, but still migrated more than the Vector (1.5-fold; Fig. 3F and G, both comparisons $P < 0.05$). The same trends for cell migration were also observed in PC3 cells (Supplementary Fig. S6).

Cancer cell migration and invasion entail the ability of malignant cells to exercise contractile force upon their surroundings (37). Using traction microscopy (13, 14), we interrogated the force-generating capacity of single Myc-CaP and PC3 cells overexpressing Twist1 (Fig. 3H–J and Supplementary Fig. S7). Compared with Vector, the Twist1-overexpressing Myc-CaP and PC3 cells showed

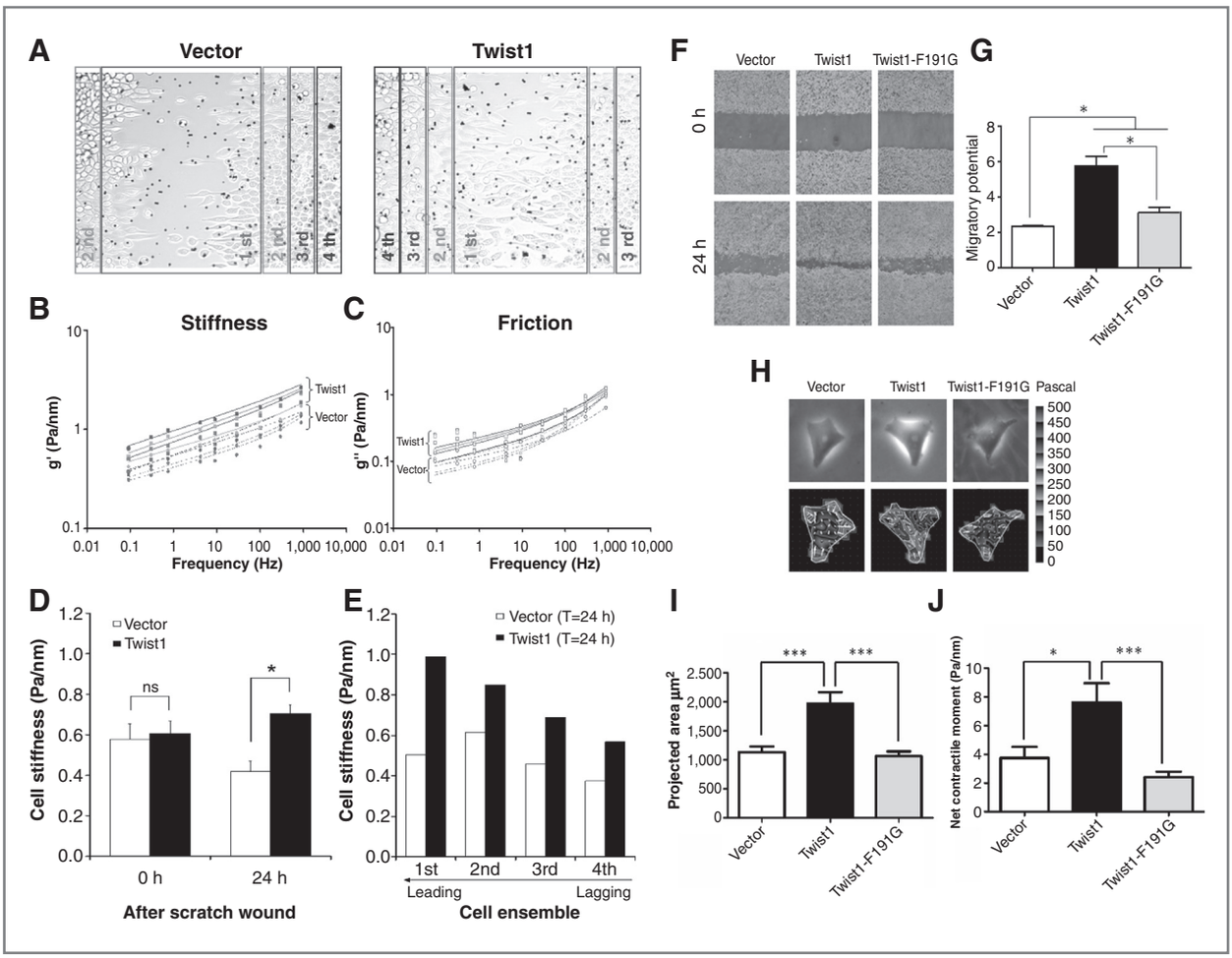

Figure 3. Twist1 overexpression induces spatiotemporal changes in the material properties of the living cytoskeleton during cellular migration of prostate cancer cells. A, representative bright fieldimages of Myc-CaP cells 24 hours after wound scratch. Using MTC, stiffness g′ (B) and loss modulus g″ (C) were measured over a physiological range of frequency (*f*). Open and closed squares represent g′ and g″ of Myc-CaP overexpressing Twist1 cells. Open and closed circles represent g′ and g″ of Vector control cells. The lines are the fit of experimental data to the structural damping equation with addition of a Newtonian viscous term as previously described (15). Fitting was carried out by non-linear regression analysis. The colors indicate the respective cell layer from the migrating front (as shown in A). Data are presented as Median (1st layer: Vector $n = 73$, Twist1 $n = 77$; 2nd layer: Vector $n = 119$, Twist1 $n = 168$: 3rd layer: Vector $n = 101$, Twist1 $n = 87$; 4th layer: Vector $n = 44$, Twist1 $n = 64$). D, stiffness of Vector and Twist1 expressing Myc-CaP cells probed at 0.75 Hz, following scratch wound (T, 0 hour) and 24 hours after. Data are presented as Geometric mean ± SE (Vector: T 0 hour $n = 169$, T 24 hours $n = 337$; Twist1: T 0 hours $n = 240$, T 24 hours $n = 396$). E, spatial distribution of cell stiffness 24 hours after making a scratch in Vector and Twist expressing Myc-CaP cells [data are presented as Median and are same as in (B)]. F, scratch wound-healing assay was conducted in Myc-CaP isogenic cell lines and representative images shown at 0 hour and 24 hours. G, relative wound closure is calculated by the remaining wound area normalized to the initial wound area ($n = 3$, 3 fields; *, $P < 0.05$ by Mann–Whitney test) by ImageJ software (NIH) and showed that Myc-CaP cells overexpressing Twist1-F191 cells were less migratory than wildtype Twist1 cells. H, Twist1 overexpression increases single prostate cancer cell traction forces on the substratum, which is attenuated by the Twist box mutation Twist1-F191G. The cell traction forces for individual cells ($n = 20$–21) is measured by using FTTM. The top panel shows representative phase contrast images of Myc-CaP isogenic cell lines. The bottom panel shows the traction maps; the colors within the cells represent the absolute magnitude of tractions in Pascals, and the arrows represent the relative magnitude and directions. I, Twist1 overexpression increases the mean of the projected area represented in bar graph format and the Twist box mutant isogenic cell line is attenuated for this phenotype. J, Twist1 overexpression increases cell traction force exerted by a single living cell, or net contractile moment, and the Twist1-F191G mutant is completely deficient for this function. Bars represent column mean; error bars are ±SEM. The values are significant by Mann–Whitney test: *, $P < 0.05$; and ***, $P < 0.001$.

increased cell spreading area and net contractile moment, a scalar measure of the cell's contractile strength (Fig. 3I and J, $P < 0.01$ both measurements and Supplementary Fig. S7B and C, $P < 0.001$ both measurements). The Twist box mutant displayed less cell spreading and lower net contractile moment compared with Twist1 (Fig. 3I and J, $P < 0.05$ for both measurements). These single-cell biophysical data corroborated our results with bulk migration assays. Collectively, these data suggested that the Twist box domain was required for increasing cytoskeletal force generation in prostate cancer cells that was associated with the full migratory potential of Twist1.

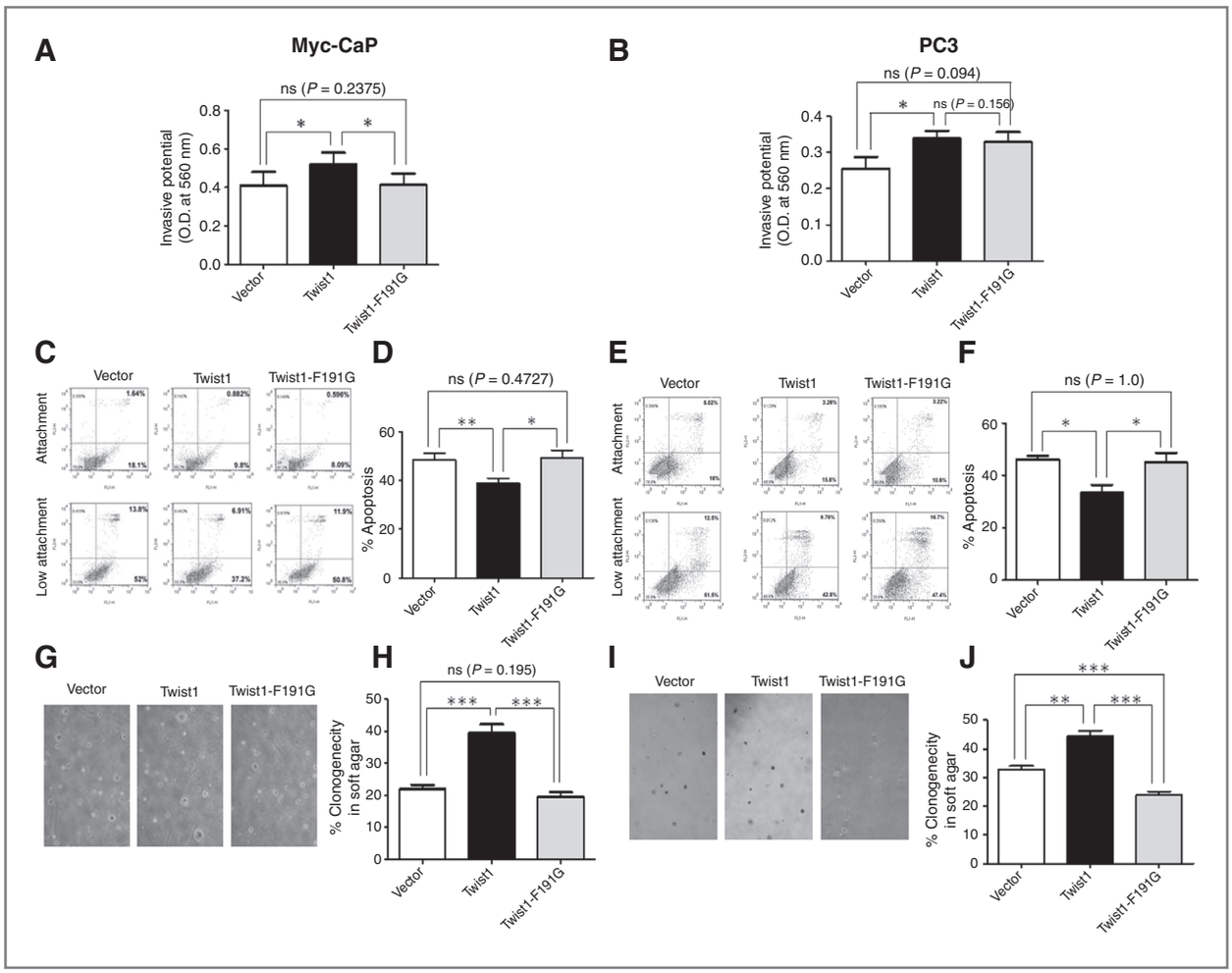

Figure 4. The Twist box mutant is defective for Twist1-induced invasion, anoikis resistance, and soft agar tumorigenicity. Transwell invasion assays with Matrigel were conducted with isogenic (A) Myc-CaP ($n = 7$) and (B) PC3 cells ($n = 6$). The Myc-CaP cells were allowed to invade for 24 hours and PC3 cells for 60 hours. Twist1 overexpression increased invasion into Matrigel for both Myc-CaP and PC3 cells, but the Twist1-F191G mutant conferred less invasive ability to these cells (represented by column mean ±SEM; *, $P < 0.05$ by Mann–Whitney test). Cells were grown adherent or in suspension using ultra-low attachment dishes. The amount of apoptotic cell death or anoikis for the ultra-low attachment conditions was quantified by AnnexinV-AlexaFluor 488 and propidium iodide staining followed by flow-cytometric analysis. Representative dot plots of (C) Myc-CaP and (E) PC3 Twist1 isogenic cell lines are shown. Percent of cells in quadrants II (early apoptotic) and III (late apoptotic) that constitute apoptotic fractions are in bold. Percent apoptosis was calculated by normalizing total apoptotic fraction in ultra-low attachment conditions to that of adherent cells and plotted as bar graph ±SEM for (D) Myc-CaP ($n = 8$) and (F) PC3 ($n = 6$) Twist1 isogenic cell lines (*, $P < 0.05$; and **, $P < 0.01$ by Student t test). A total of 5×10^5 cells were embedded in soft agar and incubated for 2 weeks. Colonies containing above 50 cells were scored in at least 5 random fields. Representative phase contrast images of (G) Myc-CaP and (I) PC3 Twist1 isogenic cell lines at ×40 magnifications are shown. The percent clonogenicity in soft agar is calculated by normalizing the number of colonies to the total number of cells and represented as bar graphs ±SEM for (H) Myc-CaP ($n = 6$) and (J) PC3 ($n = 6$; *, $P < 0.05$; **, $P < 0.01$; and ***, $P < 0.001$ by Mann–Whitney test).

The Twist box is required for Twist1-induced prostate cancer invasion, cell death resistance, and anchorage-independent growth *in vitro*

Both Myc-CaP and PC3 cells overexpressing Twist1 showed an increased invasiveness compared with Vector control cells using a Matrigel-coated Transwell invasion assay (Fig. 4A and B, both $P < 0.05$). The Twist box mutant was completely defective for invasion in Myc-CaP cells compared with Twist1 wild-type (Fig. 4A, $P < 0.05$) and trended toward being less invasive in PC3 cells (Fig. 4B, $P = 0.156$). Similar to motility, the Twist box is at least partially required for Twist1-induced prostate cancer invasion.

The resistance to anoikis facilitates metastasis of cancer cells to distant organs. Both Twist1-overexpressing Myc-CaP and PC3 cells showed decreased apoptosis when grown in suspension compared with their isogenic Vector control cells (Fig. 4C–F, both cell lines $P < 0.05$). The Twist1-F191G mutant in Myc-CaP and PC3 cells were similar to their isogenic Vector control cells (Fig. 4C–F, both cells $P > 0.47$) for anoikis resistance. We also observed that the Twist box was required to confer radioresistance

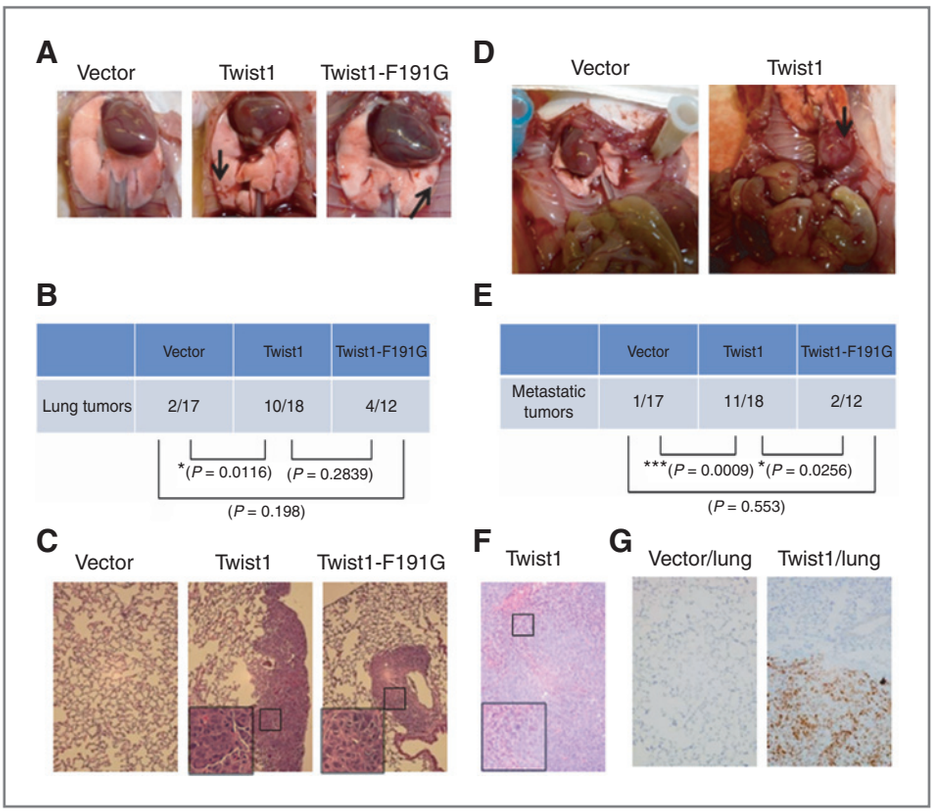

Figure 5. Twist1 overexpression confers metastatic ability to Myc-CaP prostate cancer cells *in vivo* that is dependent on the Twist box domain. The experimental lung metastasis assay was conducted with Myc-CaP Twist1 isogenic cell lines. A total of 5×10^5 cells were tail vein injected into 8-week-old athymic nude male mice, sacrificed 4 weeks later and inspected for lung colonization and extrathoracic metastases. Cohorts of 4 to 6 mice were used for each cell line and experiments were carried out three times. A, representative necropsy photographs of the lungs with lung tumors distinguished by black arrows. B, a table comparing the ability of the three isogenic cell lines to colonize lung tumors *in vivo* from (A). Twist1-overexpressing Myc-CaP cells are able to form macroscopic lung tumors *in vivo* in a much higher frequency of mice (10/18 or 55.6%) than Vector control cells (2/17 or 11.8%; $P = 0.0116$ by Fisher exact test). The Twist1 box mutant Myc-CaP cells had an intermediate phenotype *in vivo* (4/12 or 33.3% of mice; $P = 0.198$ compared with Vector and $P = 0.2839$ compared with wild-type Twist1 by Fisher exact test). C, representative hematoxylin and eosin (H&E) images of lung samples from A with insets showing magnified views of lung tumors. D, representative necropsy photographs of extrathoracic metastases from mice injected with Twist1 isogenic cells with metastases indicated by black arrows. These extrathoracic metastases represent the consequence of prostate cancer cells undergoing the full metastatic pathway following tail vein injection. E, a table comparing the ability of the three isogenic Myc-CaP cell lines to form extrathoracic metastases from D. Twist1 overexpression conferred Myc-CaP cells with the ability to form extrathoracic metastases at a higher frequency in mice (11/18 or 61.1%) than Vector control cells (1/17 or 5.9%) and the Twist1 box mutant overexpressing cells (2/12 or 16.7%; $P = 0.0009$ for Twist1 vs. Vector and $P = 0.0256$ for Twist1 vs. Twist1-F191G by Fisher exact test). F, representative H&E image of a Twist1-induced extrathoracic metastasis with the inset showing a magnified image. G, representative anti-Myc immunohistochemical images of lungs isolated from mice tail vein injected with Myc-CaP + Vector cells (left) or Myc-CaP + Twist1 cells (right). The lung tumor (and extrathoracic metastases not shown) stained positive for c-Myc, confirming the tumor cells were Myc-CaP cells.

to prostate cancer cells (Supplementary Fig. S8). Altogether, these data show that Twist1 overexpression can confer resistance to multiple cell death stimuli, and that the Twist box domain is required for these Twist1 activities in prostate cancer cells.

The *in vitro* anchorage-independent growth of Myc-CaP and PC3 cells stably overexpressing Twist1 and the Twist box mutant was conducted (Fig. 4G–J). Both Twist1-overexpressing Myc-CaP and PC3 cells showed increased frequency of colonies in soft agar compared with their isogenic Vector control cells (Fig. 4G–J, both cells $P < 0.01$). In addition, Myc-CaP cells overexpressing Twist1 had colonies of larger size (Fig. 4G). Myc-CaP and PC3 Twist box mutant cells had a similar frequency of colonies in soft agar compared with their isogenic Vector control cells (Fig. 4G–J, both cells $P>0.20$). These general results were repeated and confirmed in a third prostate cancer cell line, 22Rv1, stably overexpressing Twist1 and Twist1-F191G (Supplementary Fig. S9). These data further confirm the importance of the Twist box domain for aggressive *in vitro* prostate cancer cell behavior induced by Twist1.

The Twist box is required for Twist1-induced prostate cancer metastasis *in vivo*

Using a subcutaneous tumor graft assay, we did not observe Twist1 or Twist1-F191G overexpression increasing the *in vivo* primary tumorigenic potential or primary tumor

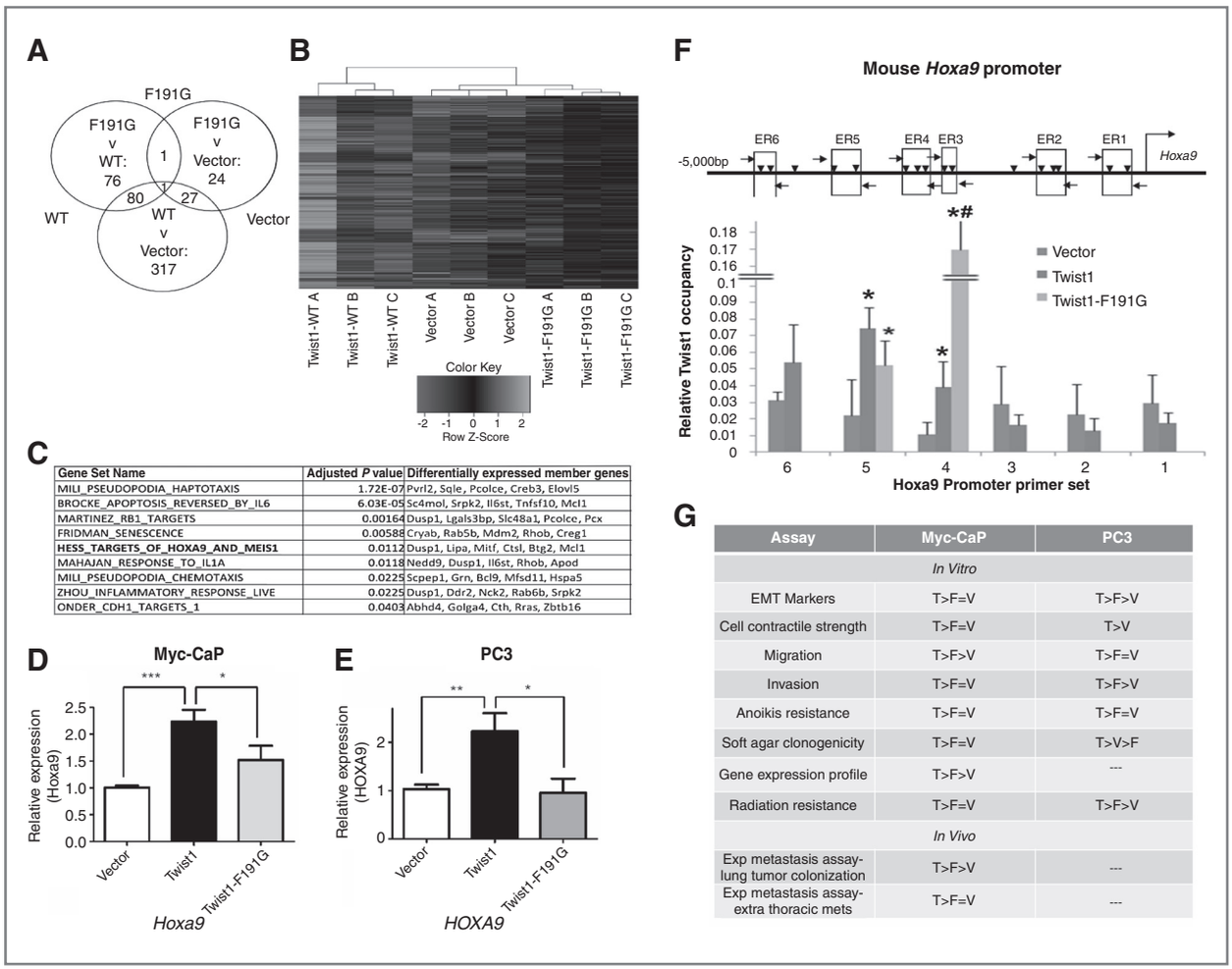

Figure 6. The Twist1 global gene expression profile in Myc-CaP prostate cancer cells is greatly attenuated by a mutation in the Twist1 box domain. A, gene expression analysis of Myc-CaP cells stably expressing Vector, Twist1 (WT), and Twist1-F191G by microarray revealed a larger set of genes that were differentially expressed between Twist1-overexpressing cells and Vector control compared with the Twist1-F191G–mutant and Vector control cells. Gene expression between groups was conducted by empirical Bayesian moderated ANOVA, and genes were considered differentially expressed if B > 0 following Benjamini–Hochberg false discovery rate (FDR). B, heatmap visualization of supervised clustering analysis of gene expression from Myc-CaP cells expressing Vector, Twist1 (WT), and Twist-1-F191G show that the Twist1 box mutant Twist1-F191G has a gene expression profile more similar to the Vector control cells. Each column represents a Myc-CaP microarray sample, and each row represents median-centered expression values for a single gene. High expression is indicated in dark grey, intermediate expression in black, and low expression in light grey. C, selected gene sets from the curated Molecular Signatures database that were overrepresented ($P < 0.05$, one-way Fisher exact test, Benjamini–Hochberg FDR) in the set of genes differentially regulated by Twist1 but not by Twist1-F191G that are relevant to phenotypic differences between prostate cancer cells overexpressing Twist1 versus Twist1-F191G as shown in this study (relative overexpression is indicated in green and relative repression by red). Twist1 but not Twist1-F191G overexpression resulted in *Hoxa9*/*HOXA9* overexpression in (D) Myc-CaP and (E) PC3 cells (*, $P < 0.05$; **, $P < 0.01$; and ***, $P < 0.001$ by Mann–Whitney test). F, schematic of the promoter region of *Hoxa9* with E-box containing regions (ER). Twist1 and Twist1-F191G bind to ER4 and ER5 by ChIP-qPCR. Inverted triangles are E-box sequences and arrows represent qPCR oligo sets flanking each ER. * indicates $P < 0.05$ as compared with Vector; and # indicates $P < 0.05$ as compared with Twist1. G, summary of phenotypes for Twist1 and the Twist box mutant in Myc-CaP and PC3 prostate cancer cells. T, Twist1; F, Twist1-F191G mutant; and V, Vector control.

growth of Myc-CaP, PC3, or 22Rv1 cells (Supplementary Fig. S10). The metastatic potential of Twist1 and Twist1-F191G–overexpressing Myc-CaP cells was assessed using the experimental lung metastasis assay. Twist1 overexpression significantly increased the ability of Myc-CaP cells to colonize the lungs and form macroscopic metastases *in vivo* (Fig. 5A and B; 10/18 mice with Twist1-overexpressing Myc-CaP cells vs. 2/17 mice with isogenic Vector control cells, $P = 0.0116$). The Twist box mutant overexpressing Myc-CaP cells lost some potential to form macroscopic lung metastases *in vivo* and had an intermediate phenotype to Vector and Twist1 Myc-CaP cells (Fig. 5B; 4/12 mice with Twist1-F191G–overexpressing Myc-CaP cells, $P>0.2$). The tumor cell morphology from Twist1 and Twist1-F191G–overexpressing cells was not different (Fig. 5C). Interestingly, mice injected tail vein with Twist1-overexpressing Myc-CaP cells showed extrathoracic metastases to distant subcutaneous tissues, abdominal organs, and distant lymph nodes

(Fig. 5D–F). Cells injected in the venous circulation seed the lungs and therefore must undergo the full metastatic pathway to produce extrathoracic metastases. Twist1 overexpression significantly increased the frequency of mice with extrathoracic metastases (Fig. 5E; 11/18 mice with Twist1-overexpressing Myc-CaP cells compared with 1/17 mice with isogenic Vector control cells, $P = 0.0009$). The Twist box was required for Myc-CaP cells to undergo the full metastatic pathway and give rise to extrathoracic metastases (Fig. 6E; 2/12 mice injected with Twist1-F191G–overexpressing Myc-CaP cells, $P = 0.0256$ compared with Twist1; and $P = 0.553$ compared with Vector control cells). The Myc-CaP identity of lung tumors and extrathoracic metastases was confirmed by Myc IHC (Fig. 5G). These results show that the Twist box domain is required for Twist1-induced metastasis of prostate cancer cells *in vivo*.

Gene expression profiling reveals *Hoxa9* as a direct target of Twist1 that is partially required for Twist1-induced prometastatic phenotypes

Global gene expression analysis on the isogenic Myc-CaP lines revealed several genes differentially expressed in each pairwise comparison. Compared with Vector control, Twist1 overexpression altered the expression of 424 genes. Twist1-F191G overexpression compared against Vector control altered the expression of much fewer genes, 53 genes, and the majority (28/53) of these genes were also observed with Twist1 overexpression. Between Twist1 and Twist1-F191G, 158 genes were altered, of which the majority were also altered in Twist1 (81/158; Fig. 6A and Supplementary Tables S1 and S2). This expression pattern is consistent with Twist1-F191G having a greatly attenuated transcriptional program compared with wild-type Twist1 (Fig. 6B). These global gene expression profiling data are consistent with our promoter reporter assays conducted above suggesting that the Twist box domain is required for the full transcriptional activity of Twist1 (Fig. 2B and Supplementary Fig. S1). These findings are highly suggestive of a transcriptional mechanism for the phenotypic differences observed between prostate cancer cells overexpressing Twist1 and those overexpressing the Twist box mutant.

GSEA (38) was used to identify gene sets which were overrepresented in Twist1 but not Twist1-F191G. Many of the overrepresented gene sets were related to phenotypes which we directly assayed, aggressive cellular behavior and metastasis, and were observed with overexpression of Twist1 but not Twist1-F191G (Fig. 6C). One gene set of interest was directed by the homeobox transcription factor, Hoxa9, which is strongly implicated in leukemogenesis. Furthermore, the Hox homolog HOXA5 had been shown previously to interact physically with Twist and antagonize repression of p53 to genotoxic stressors. Thus, we confirmed our microarray data by qPCR and Western blotting showing that Twist1 overexpression resulted in *Hoxa9*/*HOXA9* overexpression in Myc-CaP and PC3 (Fig. 6D and E; both $P < 0.01$ by qPCR and Supplementary Fig. S11A and S11B by Western blotting). Twist1 also bound to the *Hoxa9* promoter in a region containing canonical E-box sequences as shown by ChIP-qPCR (Fig. 6F). Consistent with our global gene expression data, the Twist box mutant was unable to upregulate the expression of *Hoxa9*/*HOXA9* overexpression in Myc-CaP and PC3 and was similar to Vector control (Fig. 6D and E; both $P < 0.05$ by qPCR and Supplementary Fig. S11A and S11B by Western blotting). However, the Twist1-F191G mutant was still capable of binding to the *Hoxa9* promoter by ChIP-qPCR, suggesting that the Twist box was required for the full transcriptional activity of Twist1 (Fig. 6F and summarized differences between *in vitro* and *in vivo* phenotypes of Twist1 and Twist1-F191G in Fig. 6G).

Interestingly, we found that many of the *in vitro* prometastatic phenotypes of Twist1 overexpression in Myc-CaP cells were significantly blunted following short hairpin RNA (shRNA)-mediated knockdown of *Hoxa9* (Fig. 7). Three separate shRNA constructs against *Hoxa9* were each able to knockdown Hoxa9 mRNA and protein expression in Myc-CaP cells overexpressing Twist1 (Fig. 7A; $P < 0.05$ for qPCR). *Hoxa9* knockdown in these Twist1-overexpressing cells resulted in a reduction in Twist1-induced cellular migration, invasion, anoikis resistance, and soft agar clonogenicity (Fig. 7B–G; $P < 0.05$ all at least). Collectively, these data suggest that Twist1 imparts prometastatic phenotypes on prostate cancer cells, in part, by directly upregulating *Hoxa9* expression.

Discussion

Our study shows that Twist1 overexpression in prostate cancer cells induces an EMT phenotype, augments migration, invasion, and resistance to anoikis and metastasis. We show that the highly conserved Twist box domain is required for many of these properties of Twist1 associated with aggressive tumor cell behavior *in vitro* and most importantly for metastasis *in vivo*. We also show that the Twist box domain is required for the full transcriptional activity of Twist1 and facilitates these prometastatic cellular functions by directing specific transcriptional programs. We show that Twist1 directly regulates the transcriptional prometastatic target, *Hoxa9*, which is at least partially required for Twist1-induced prometastatic phenotypes in prostate cancer cells.

The Twist box is highly conserved among vertebrates and is critical for the role of Twist1 in development as shown by inactivating mutations in this region of the human gene resulting in the Saethre–Chotzen syndrome, characterized primarily by craniosynostosis (5, 39). Consistent with humans, the Charlie Chaplin mouse strain with craniosynostosis and hind-limb abnormalities results from a S192P substitution mutation in the Twist box domain (40). Mechanistically, Twist1 binds to the Runx2 transcription factor via the Twist box and inhibits the Runx2 transcriptional program necessary for osteoblast differentiation. Similarly, Twist1 binds Sox9 via the Twist box and inhibits Sox9-dependent transcriptional programs required for chondrocyte differentiation (41). Twist1 may also directly modulate transcription of target genes, and the Twist box was shown to be both necessary and sufficient for this transactivation activity (34). The Twist box transactivation domain likely

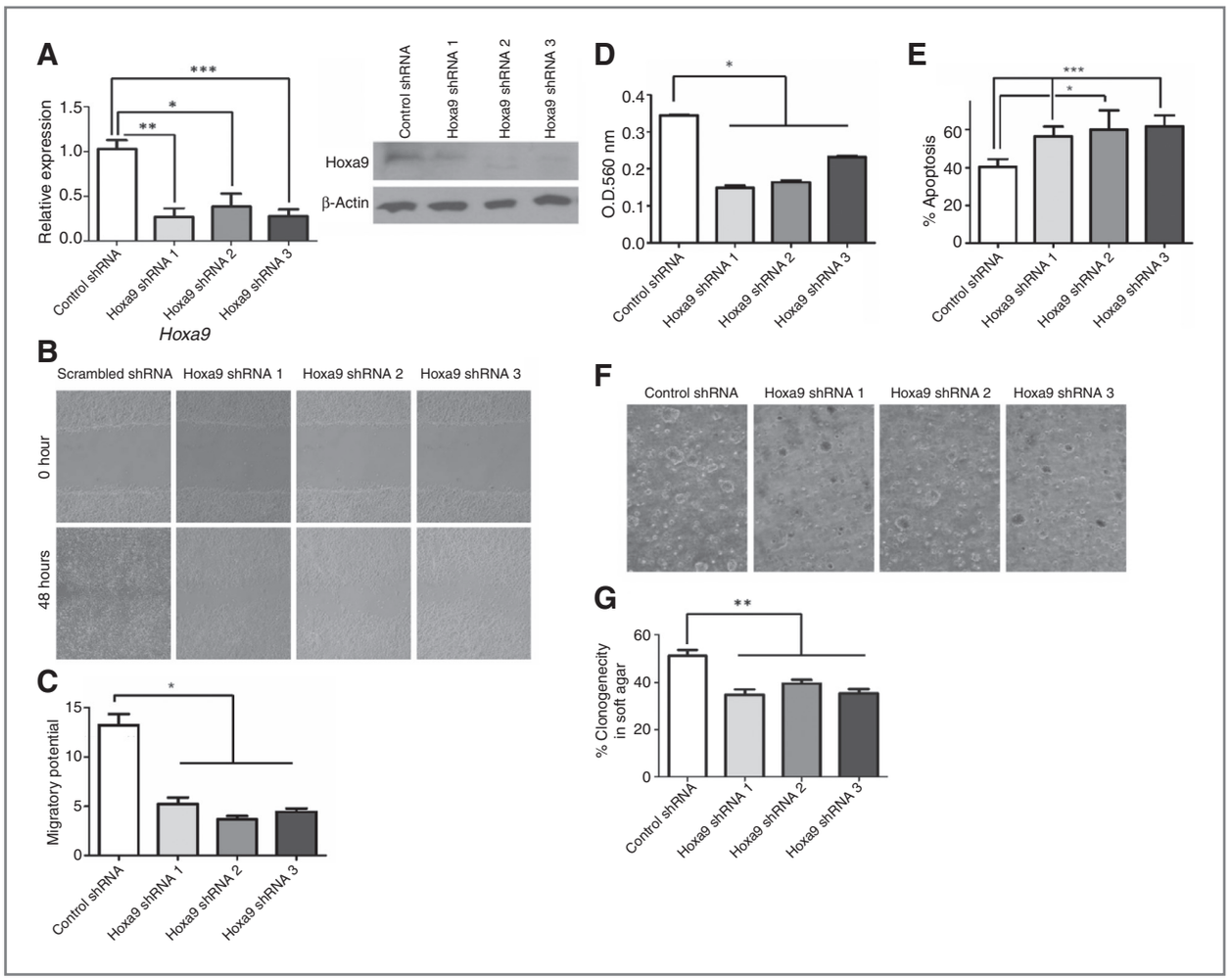

Figure 7. *Hoxa9* is partly required for Twist1-induced migration, invasion, anoikis resistance, and soft agar tumorigenicity of Myc-CaP cells. A, Myc-CaP cell stably overexpressing Twist1 were transduced with shRNA constructs against *Hoxa9* or scrambled control and relative expression determined by *Hoxa9* qPCR (left, $n \geq 3$) and Hoxa9 Western blotting (right). B, scratch wound-healing assay of Myc-CaP + Twist1 isogenic cell lines and representative images shown at 0hour and 48 hours. C, in relative wound closure calculations (as in Fig. 3; all $n = 3$, 3 fields per experiment). D, Transwell invasion assays with Matrigel were conducted with isogenic Myc-CaP + Twist1 cells ($n = 6$, represented by column mean ±SEM). E, cells were grown adherent or in suspension using ultra-low attachment dishes and anoikis quantified by AnnexinV- AlexaFluor 488 and propidium iodide staining (as in Fig. 4) plotted as bar graphs ±SEM. A total of 5×10^5 cells were embedded in soft agar and incubated for 2 weeks. Colonies containing above 50 cells were scored in at least 5 random fields. F, representative phase contrast images ×40 magnifications are shown. G, the percent clonogenicity in soft agar is calculated by normalizing the number of colonies to the total number of cells and represented as bar graphs ±SEM ($n \geq 4$). All comparisons, *, $P < 0.05$; **, $P < 0.01$; and ***, $P < 0.001$ by Mann–Whitney test.

adopts an α-helical structure, and the three amino acids, Leu-187, Phe-191, Arg-195, are essential for transactivation function and may occupy the same three-dimensional surface of this α-helix. Twist1 has been shown to directly upregulate the expression of several target genes important for cancer progression like *Akt2* expression, which enhances cell migration, invasion, and resistance to chemotherapy (42). In agreement with these findings in breast cancer, our expression profiling of Twist1-overexpressing prostate cancer cells were similar to gene signatures consistent with increased cell migration, invasion, and resistance to apoptosis. However, whether the Twist box mediates a transcriptional program required for Twist1-induced metastasis in prostate cancer cells by actively inhibiting another transcription factor or by directly regulating downstream target genes requires further study.

The role of the Twist box in cancer-related functions has only recently been appreciated. In a recent study, the Twist box was required for Twist1 binding to the NF-κB subunit RELA to activate transcriptional activity, increased DNA-binding affinity to the interleukin 8 (IL-8) promoter and transcriptional activation that was required for breast cancer cell invasion *in vitro* (43). We did not observe direct Twist box-dependent regulation of IL-8 by Twist1 in our system, but in agreement with this study, we did observe Twist box-dependent gene sets consistent with NF-κB–regulated inflammatory genes. The Twist box has also recently been shown to bind p53 and induce destabilization via MDM2-

mediated degradation in sarcoma cells (44). This mechanism is separate from Twist1 indirect regulation of p53 by modulating the ARF/MDM2/p53 pathway (45). We do not believe that Twist box-dependent p53 regulation explains the Twist1-induced metastatic phenotypes we observed in prostate cancer cells as PC3 cells are *TP53*-null and a similar Twist1-F191L substitution mutation in the Twist box did not affect Twist1-p53 interaction (44). Our study findings require validation in other cancer histologies before our results can be generalized further and confirmation using autochthonous transgenic models of tumorigenesis and spontaneous metastasis models is needed. Despite these limitations, our current study confirms the recent *in vitro* data showing the importance of the Twist box domain for the protumorigenic activities of Twist1. Importantly, our study shows for the first time the requirement of the Twist box for the prometastatic functions of Twist1 *in vitro* and *in vivo*.

TWIST1 expression levels seem to be correlated with prostate cancer aggressiveness and factors associated with lethal metastatic disease (Fig. 1; refs. 7, 33). The downregulation of Twist1 in androgen-independent prostate cancer cells increased their sensitivity to anticancer drugs and suppressed their migration and invasion abilities, suggesting Twist1 inactivation as a potential therapeutic strategy (7). TWIST1 expression during postnatal life is restricted tightly to a subpopulation of mesoderm-derived tissues, and limited studies suggest that Twist1 inhibition systemically may be well tolerated (46). Furthermore, our previous study suggested that suppression of Twist1 to physiologic levels *in vivo* is sufficient for anticancer effects (11). However, the direct inhibition of Twist1 as a therapeutic maneuver still poses a few potential challenges. First, Twist1 is a pleiotropic transcription factor essential for mammalian development (47). Second, bHLH transcription factors have been difficult to target directly with small molecules (48). A solution to these issues is dissecting what are the critical domains of Twist1 and what are the crucial Twist1 downstream transcriptional targets that are required for Twist1-dependent tumorigenicity and prometastatic functions.

Using comparative gene expression profiling of Twist1 and Twist box mutant cells, we discovered *Hoxa9* as a novel direct gene target of Twist1 that was required, in part, for many Twist1-induced prostate cancer prometastatic phenotypes *in vitro*. Although there is a rich literature on the oncogenic role of Hoxa9 in leukemia (49), only one recent report has suggested a role for *Hoxa9* in prostate cancer (50). Thus, we have uncovered a novel mechanism involving Twist1 and Hoxa9 oncoproteins collaborating to facilitate prostate cancer progression and metastatic cellular behavior.

In conclusion, these data herein have increased our insight into the structure–function relationships of the Twist1 oncoprotein in cancer and point to the Twist box as a critical domain required for directing transcriptional prometastatic programs in prostate cancer cells. Our findings suggest therapeutic measures against TWIST1-overexpressing prostate cancer cells should be minimally directed against the Twist box domain and Twist1-regulated transcriptional targets such as *Hoxa9*.

Disclosure of Potential Conflicts of Interest

No potential conflicts of interest were disclosed.

Authors' Contributions

Conception and design: S.T. Chettiar, T.F. Burns, R.K. Hales, S.S. An, P.T. Tran
Development of methodology: R.P. Gajula, S.T. Chettiar, S.S. An, P.T. Tran
Acquisition of data (provided animals, acquired and managed patients, provided facilities, etc.): R.P. Gajula, S.T. Chettiar, R.D. Williams, S. Thiyagarajan, R. Wang, N. Gandhi, A.T. Wild, F. Vesuna, J. Ma, T. Salih, T.F. Burns, C.H. Chung, S.S. An, P.T. Tran
Analysis and interpretation of data (e.g., statistical analysis, biostatistics, computational analysis): R.P. Gajula, S.T. Chettiar, R.D. Williams, S. Thiyagarajan, K. Aziz, R. Wang, N. Gandhi, A.T. Wild, J. Ma, E. Fertig, S. Biswal, C.H. Chung, R.K. Hales, S.S. An, P.T. Tran
Writing, review, and/or revision of the manuscript: R.P. Gajula, S.T. Chettiar, Y. Kato, K. Aziz, N. Gandhi, A.T. Wild, F. Vesuna, J. Cades, E. Fertig, T.F. Burns, C.H. Chung, C.M. Rudin, J.M. Herman, R.K. Hales, S.S. An, P.T. Tran
Administrative, technical, or material support (i.e., reporting or organizing data, constructing databases): R.P. Gajula, S.T. Chettiar, Y. Kato, K. Aziz, N. Gandhi, V. Raman, P.T. Tran
Study supervision: P.T. Tran

Grant Support

This work was funded by RSNA Research Medical Student Grant (A.T. Wild), Johns Hopkins Laboratory Radiation Oncology Training Fellow NIH-T32CA121937 (to R.D. Williams), NIH P50CA103175 and U54CA141868 (to S.S. An), and Phyllis and Brian L. Harvey Scholar Award from Patrick C. Walsh Prostate Cancer Research Fund, DoD Prostate Cancer Physician Research Training Award W81XWH-11-1-0272, ACS Scholar 122688-RSG-12-196-01-TBG, and the NIH P50CA103175 and R01CA166348 (to P.T. Tran).

The costs of publication of this article were defrayed in part by the payment of page charges. This article must therefore be hereby marked *advertisement* in accordance with 18 U.S.C. Section 1734 solely to indicate this fact.

Received April 30, 2013; revised August 7, 2013; accepted August 9, 2013; published OnlineFirst August 27, 2013.

References

1. Siegel R, Naishadham D, Jemal A. Cancer statistics, 2012. CA Cancer J Clin 2012;62:10–29.
2. Pound CR, Partin AW, Eisenberger MA, Chan DW, Pearson JD, Walsh PC. Natural history of progression after PSA elevation following radical prostatectomy. Jama 1999;281:1591–7.
3. Thiery JP, Acloque H, Huang RY, Nieto MA. Epithelial-mesenchymal transitions in development and disease. Cell 2009;139:871–90.
4. Ansieau S, Morel AP, Hinkal G, Bastid J, Puisieux A. TWISTing an embryonic transcription factor into an oncoprotein. Oncogene 2010;29:3173–84.
5. Qin Q, Xu Y, He T, Qin C, Xu J. Normal and disease-related biological functions of Twist1 and underlying molecular mechanisms. Cell Res 2011;22:90–106.
6. Kwok WK, Ling MT, Lee TW, Lau TC, Zhou C, Zhang X, et al. Up-regulation of TWIST in prostate cancer and its implication as a therapeutic target. Cancer Res 2005;65:5153–62.
7. Shiota M, Yokomizo A, Tada Y, Inokuchi J, Kashiwagi E, Masubuchi D, et al. Castration resistance of prostate cancer cells caused by castration-induced oxidative stress through Twist1 and androgen receptor overexpression. Oncogene 2010;29:237–50.
8. Shiota M, Zardan A, Takeuchi A, Kumano M, Beraldi E, Naito S, et al. Clusterin mediates TGF-beta-induced epithelial-mesenchymal transition and metastasis via Twist1 in prostate cancer cells. Cancer Res 2012;72:5261–72.
9. Xie D, Gore C, Liu J, Pong RC, Mason R, Hao G, et al. Role of DAB2IP in modulating epithelial-to-mesenchymal transition and

prostate cancer metastasis. Proc Natl Acad Sci U S A 2010;107: 2485–90.
10. Watson PA, Ellwood-Yen K, King JC, Wongvipat J, Lebeau MM, Sawyers CL. Context-dependent hormone-refractory progression revealed through characterization of a novel murine prostate cancer cell line. Cancer Res 2005;65:11565–71.
11. Tran PT, Shroff EH, Burns TF, Thiyagarajan S, Das ST, Zabuawala T, et al. Twist1 suppresses senescence programs and thereby accelerates and maintains mutant kras-induced lung tumorigenesis. PLoS Genet 2012;8:e1002650.
12. Garzon-Muvdi T, Schiapparelli P, ap Rhys C, Guerrero-Cazares H, Smith C, Kim DH, et al. Regulation of brain tumor dispersal by NKCC1 through a novel role in focal adhesion regulation. PLoS Biol 2012;10: e1001320.
13. Butler JP, Tolic-Norrelykke IM, Fabry B, Fredberg JJ. Traction fields, moments, and strain energy that cells exert on their surroundings. Am J Physiol 2002;282:C595–605.
14. Wang N, Tolic-Norrelykke IM, Chen J, Mijailovich SM, Butler JP, Fredberg JJ, et al. Cell prestress. I. Stiffness and prestress are closely associated in adherent contractile cells. Am J Physiol 2002; 282:C606–16.
15. Fabry B, Maksym GN, Butler JP, Glogauer M, Navajas D, Fredberg JJ. Scaling the microrheology of living cells. Phys Rev Lett 2001;87:148102.
16. An SS, Fabry B, Trepat X, Wang N, Fredberg JJ. Do biophysical properties of the airway smooth muscle in culture predict airway hyperresponsiveness? Am J Respir Cell Mol Biol 2006;35:55–64.
17. Tran PT, Fan AC, Bendapudi PK, Koh S, Komatsubara K, Chen J, et al. Combined inactivation of MYC and K-Ras oncogenes reverses tumorigenesis in lung adenocarcinomas and lymphomas. PLoS ONE 2008;3: e2125.
18. Fiucci G, Ravid D, Reich R, Liscovitch M. Caveolin-1 inhibits anchorage-independent growth, anoikis and invasiveness in MCF-7 human breast cancer cells. Oncogene 2002;21:2365–75.
19. Zeng J, See AP, Aziz K, Thiyagarajan S, Salih T, Gajula RP, et al. Nelfinavir induces radiation sensitization in pituitary adenoma cells. Cancer Biol Ther 2011;12:657–63.
20. Lapointe J, Li C, Higgins JP, van de Rijn M, Bair E, Montgomery K, et al. Gene expression profiling identifies clinically relevant subtypes of prostate cancer. Proc Natl Acad Sci U S A 2004;101:811–6.
21. Arredouani MS, Lu B, Bhasin M, Eljanne M, Yue W, Mosquera JM, et al. Identification of the transcription factor single-minded homologue 2 as a potential biomarker and immunotherapy target in prostate cancer. Clin Cancer Res 2009;15:5794–802.
22. Magee JA, Araki T, Patil S, Ehrig T, True L, Humphrey PA, et al. Expression profiling reveals hepsin overexpression in prostate cancer. Cancer Res 2001;61:5692–6.
23. Yu YP, Landsittel D, Jing L, Nelson J, Ren B, Liu L, et al. Gene expression alterations in prostate cancer predicting tumor aggression and preceding development of malignancy. J Clin Oncol 2004;22: 2790–9.
24. Welsh JB, Sapinoso LM, Su AI, Kern SG, Wang-Rodriguez J, Moskaluk CA, et al. Analysis of gene expression identifies candidate markers and pharmacological targets in prostate cancer. Cancer Res 2001;61: 5974–8.
25. Vanaja DK, Cheville JC, Iturria SJ, Young CY. Transcriptional silencing of zinc finger protein 185 identified by expression profiling is associated with prostate cancer progression. Cancer Res 2003;63:3877–82.
26. Varambally S, Yu J, Laxman B, Rhodes DR, Mehra R, Tomlins SA, et al. Integrative genomic and proteomic analysis of prostate cancer reveals signatures of metastatic progression. Cancer Cell 2005;8:393–406.
27. Taylor BS, Schultz N, Hieronymus H, Gopalan A, Xiao Y, Carver BS, et al. Integrative genomic profiling of human prostate cancer. Cancer Cell 2010;18:11–22.
28. Singh D, Febbo PG, Ross K, Jackson DG, Manola J, Ladd C, et al. Gene expression correlates of clinical prostate cancer behavior. Cancer Cell 2002;1:203–9.
29. Luo JH, Yu YP, Cieply K, Lin F, Deflavia P, Dhir R, et al. Gene expression analysis of prostate cancers. Mol Carcinog 2002;33:25–35.
30. Liu P, Ramachandran S, Ali Seyed M, Scharer CD, Laycock N, Dalton WB, et al. Sex-determining region Y box 4 is a transforming oncogene in human prostate cancer cells. Cancer Res 2006;66: 4011–9.
31. LaTulippe E, Satagopan J, Smith A, Scher H, Scardino P, Reuter V, et al. Comprehensive gene expression analysis of prostate cancer reveals distinct transcriptional programs associated with metastatic disease. Cancer Res 2002;62:4499–506.
32. Wallace TA, Prueitt RL, Yi M, Howe TM, Gillespie JW, Yfantis HG, et al. Tumor immunobiological differences in prostate cancer between African-American and European-American men. Cancer Res 2008;68: 927–36.
33. Yuen HF, Chua CW, Chan YP, Wong YC, Wang X, Chan KW. Significance of TWIST and E-cadherin expression in the metastatic progression of prostatic cancer. Histopathology 2007;50:648–58.
34. Laursen KB, Mielke E, Iannaccone P, Fuchtbauer EM. Mechanism of transcriptional activation by the proto-oncogene Twist1. J Biol Chem 2007;282:34623–33.
35. Vesuna F, van Diest P, Chen JH, Raman V. Twist is a transcriptional repressor of E-cadherin gene expression in breast cancer. Biochem Biophys Res Commun 2008;367:235–41.
36. Chaffer CL, Weinberg RA. A perspective on cancer cell metastasis. Science 2011;331:1559–64.
37. Mierke CT, Rosel D, Fabry B, Brabek J. Contractile forces in tumor cell migration. Eur J Cell Biol 2008;87:669–76.
38. Subramanian A, Tamayo P, Mootha VK, Mukherjee S, Ebert BL, Gillette MA, et al. Gene set enrichment analysis: a knowledge-based approach for interpreting genome-wide expression profiles. Proc Natl Acad Sci U S A 2005;102:15545–50.
39. Howard TD, Paznekas WA, Green ED, Chiang LC, Ma N, Ortiz de Luna RI, et al. Mutations in TWIST, a basic helix-loop-helix transcription factor, in Saethre-Chotzen syndrome. Nat Genet 1997;15: 36–41.
40. Bialek P, Kern B, Yang X, Schrock M, Sosic D, Hong N, et al. A twist code determines the onset of osteoblast differentiation. Dev Cell 2004;6:423–35.
41. Gu S, Boyer TG, Naski MC. Basic helix-loop-helix transcription factor Twist1 inhibits transactivator function of master chondrogenic regulator Sox9. J Biol Chem 2012;287:21082–92.
42. Cheng GZ, Chan J, Wang Q, Zhang W, Sun CD, Wang LH. Twist transcriptionally upregulates AKT2 in breast cancer cells leading to increased migration, invasion, and resistance to paclitaxel. Cancer Res 2007;67:1979–87.
43. Li S, Kendall SE, Raices R, Finlay J, Covarrubias M, Liu Z, et al. TWIST1 associates with NF-kappaB subunit RELA via carboxyl-terminal WR domain to promote cell autonomous invasion through IL8 production. BMC Biol 2012;10:73.
44. Piccinin S, Tonin E, Sessa S, Demontis S, Rossi S, Pecciarini L, et al. A "twist box" code of p53 inactivation: twist box: p53 interaction promotes p53 degradation. Cancer Cell 2012;22:404–15.
45. Maestro R, Dei Tos AP, Hamamori Y, Krasnokutsky S, Sartorelli V, Kedes L, et al. Twist is a potential oncogene that inhibits apoptosis. Genes Dev 1999;13:2207–17.
46. Pan D, Fujimoto M, Lopes A, Wang YX. Twist-1 is a PPARdelta-inducible, negative-feedback regulator of PGC-1alpha in brown fat metabolism. Cell 2009;137:73–86.
47. Chen ZF, Behringer RR. twist is required in head mesenchyme for cranial neural tube morphogenesis. Genes Dev 1995;9:686–99.
48. Verdine GL, Walensky LD. The challenge of drugging undruggable targets in cancer: lessons learned from targeting BCL-2 family members. Clin Cancer Res 2007;13:7264–70.
49. Gough SM, Slape CI, Aplan PD. NUP98 gene fusions and hematopoietic malignancies: common themes and new biologic insights. Blood 2011;118:6247–57.
50. Chen JL, Li J, Kiriluk KJ, Rosen AM, Paner GP, Antic T, et al. Deregulation of a Hox protein regulatory network spanning prostate cancer initiation and progression.Clin Cancer Res 2012;18: 4291–302.